XI International Conference on Computational Plasticity. Fundamentals and Applications
COMPLAS XI
E. Oñate, D.R.J. Owen, D. Peric and B. Suárez (Eds)

AN ARBITRARY LAGRANGIAN-EULERIAN (ALE) APPROACH FOR THE MODELING OF TENSION LEVELING PROCESSES

LORENZ STEINWENDER*, ALEXANDER KAINZ*, KONRAD KRIMPELSTÄTTER† AND KLAUS ZEMAN*

*Institute of Computer-Aided Methods in Mechanical Engineering
Johannes Kepler University Linz
Altenbergerstraße 69, 4040 Linz, Austria
e-mail: lorenz.steinwender@jku.at, web page: http://came.mechatronik.uni-linz.ac.at

†Siemens VAI Metals Technologies GmbH
Turmstraße 44, 4031 Linz, Austria
e-mail: konrad.krimpelstaetter@siemens.com, web page: http://www.siemens-vai.com

Key words: Metal Forming, Tension Leveling, Arbitrary Lagrangian-Eulerian (ALE), Principle of Virtual Work

Abstract. Strip flatness and surface quality are crucial factors for the production of high-quality cold-rolled metal strip. Tension leveling (employed as one of the final steps in continuous galvanizing and finishing lines) improves strip flatness and minimizes residual stresses by inducing small elasto-plastic strip deformations, while the strip is bent under high tension stresses around multiple rolls with small diameters.

Simulations of tension leveling processes employing commercial Finite Element software packages yield unacceptable computational costs: The small and coupled elasto-plastic deformations occur simultaneously at concentrated regions along the strip bending line and steady-state solutions cannot be reached before at least one strip cross-section has passed through the entire process unit of the tension leveler.

In order to overcome these critical aspects, a new and alternative modeling approach, based on the principle of virtual work and on a specialized "Arbitrary Lagrangian-Eulerian" (ALE) formulation was elaborated. This novel concept utilizes "Parametric Shape Functions" (PSF) that describe both geometry and strain distribution of the deformed strip. The decoupling of the mesh movement from the material movement in the ALE description allows for the implementation of highly efficient contact algorithms, while the strip length under consideration can be minimized. Compared to (already) optimized commercial FEM-models, the PSF-model exhibits a drastic reduction of degrees of freedom and computational costs (by a factor of 100 and more in typical test cases) while high agreement of the key results is simultaneously maintained.

1 INTRODUCTION

As the demand for perfect flatness and outstanding surface properties both of hot- and cold-rolled strips rises continuously, tension leveling becomes an increasingly important process step in the production of high-class metal strip. Tension levelers are typically located at the exit of strip processing lines (for example continuous galvanizing or finishing lines) to reduce flatness deficiencies like center and edge buckles or strip camber as well as to minimize residual stresses of the finished strip. These often unacceptable quality deficiencies are the result of an inappropriate material flow inside the roll gap during hot- or cold-rolling operations or may occur due to plastic deformations after rolling (e.g. during coiling or uncoiling).

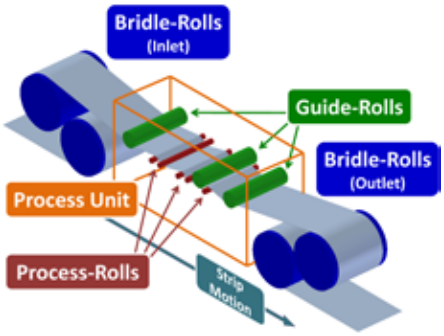

Figure 1: Typical Tension Leveler Setup.

Figure 2: Industrial Tension Leveler.

As depicted in Figure 1, a tension leveler typically consists of a set of *bridle-rolls* at the inlet and outlet (large black & yellow rolls in Figure 2) and a *process unit* (green machine block in Figure 2), which is located in-between the bridle-rolls. In this process unit the metal strip is bent alternately under high tension stresses (in the range of 5-70% of the yield strength, cp. [5]) around *guide-rolls* and *process-rolls* with particularly small diameters (both roll types are typically undriven). The combined bending and tensile stresses yield elasto-plastic strip deformations, which are comparatively small at the strip centerline (where plastic strip elongations typically do not exceed a value of about five percent), but may be locally considerably large (at the strip surfaces) due to the superimposed bending strains.

The cumulative amount of the elasto-plastic centerline strain depends strongly on the *curvature peaks* of the strip, which occur at the strip/roll contact points in typical tension leveling setups. Observations at industrial tension levelers prove that the strip will not approach the roll radii in many typical tension leveling cases – in particular when thick strip, small rolls, low strip tension, small roll adjustments, high-strength materials or high strip velocities (leading to pronounced inertial effects) are involved. In these cases, the strip will exhibit *line contact* as opposed to *surface contact* and the curvature of the strip will be smaller than the curvature of the roll in this point. The fast and precise prediction

of the actual strip curvature distribution is therefore of high relevance to a reliable design of tension leveling machines.

2 STATE OF THE ART & PROBLEM STATEMENT

First works dealing with aspects of the tension leveling process date back to the 1950s and 1960s. At that time it was common in the scientific community to assume that the strip would approach the curvature of the process-rolls in all strip/roll contact points (cp. e.g. [2]). In the early 1970s, Sheppard and Roberts [3] were among the first researchers to state that the actual bending radius of the strip in the contact point can be significantly larger than the radius of the roll. In the mid 1970s, first attempts were made to empirically predict the strip curvature at those rolls, where line contact occurs [4].

Hoffmann [5] proposed in his PhD thesis a basic, iterative model for the geometrical fitting of the strip curvature distribution in a given roll system. Applying certain simplifications and restrictions, a prediction for the shape of the strip bending line could be made for different strip dimensions, materials and roll settings.

With the emergence of sufficiently fast mainframes in the late 1990s, the Finite Element Method (FEM) allowed for the numerical determination of the strip curvature distribution. However, due to their excessive calculation times, most FEM analyses presented in the literature still require problematic trade-offs between the model's significance and the computational cost efficiency and can therefore only be used to simulate few selected tension leveling scenarios.

Nowadays, in many cases, tension leveling designs and roll adjustment strategies are based on computationally expensive but still rough offline calculation models, which have to be supplemented by trial and error procedures during the operation. In order to improve the design of tension leveling machines, precise numerical methods are essential. Key objectives of adequate models are the determination of the strip bending line, the analysis of the reaction forces at the bending rolls, the required level of tension, the tension losses due to plastic deformation as well as the power requirements of the drives (which was elaborately analyzed by the authors in an associated research project, cp. [6]).

3 CHALLENGES USING COMMERCIAL FINITE ELEMENT PACKAGES

Finite Element Models yield all key results, but require unacceptable computational costs. It could be shown in detailed analyses that both 3-D and 2-D (plane strain) simulations, and both continuum and structural modeling concepts yield comparable and reliable simulation results [7].

The numerical simulation of the tension leveling process utilizing commercial FEM packages is particularly challenging, as the strip is deformed simultaneously at different small regions along its bending line. This sequence of small elasto-plastic deformations has to be treated as a coupled whole. Hence, in a Lagrangian formulation (where mesh and material are coupled throughout the deformation process), the simulated strip has to

be several times longer than the length of the leveler's process-unit and the mesh needs to be finely discretized along this entire strip length.

Large numbers of nodes and degrees of freedom, severely non-linear contact characteristics (hard and frictionless, with frequent contact updates), a non-linear constitutive law (elasto-viscoplastic, path-dependent, including the Bauschinger effect) and large strip rotations cause unacceptable simulation runtimes (in the range of a few days for already optimized, but still significant FEM models on modern mainframes) – making such models inappropriate as efficient dimensioning tools for industrial applications.

4 PARAMETRIC SHAPE FUNCTION (PSF) MODEL

To reduce the unacceptable computational costs of FEM simulation models, a novel modeling approach was pursued. On account of an in-depth analysis of the physical correlations relevant for the tension leveling process, appropriate parametric shape functions (PSF) could be identified, which describe both the strip's geometry (i.e. its curvature) and the strain state of the centerline along the Eulerian (i.e. actual) arc length of the strip. The bending line is determined in 2-D (plane strain) employing a drastically reduced number of degrees of freedom as compared to concepts based on commercial FEM software packages (as discussed above).

5 PROPOSED ARBITRARY LAGRANGIAN-EULERIAN FORMALISM

When handling the investigated problem, the application of the Arbitrary Lagrangian-Eulerian (ALE) theory is very advantageous. In the ALE referential formulation, the mesh speed $\hat{v}$ can be chosen arbitrarily, which is a fundamental difference to both the Lagrangian material formulation (where the mesh speed equals the material speed $\rightarrow\ \hat{v} = v$) and the Eulerian spatial formulation (where the mesh speed is zero $\rightarrow\ \hat{v} = 0$).

Any arbitrary position along the bending line of a strip can be denoted in the ALE, the Lagrangian and in the Eulerian formulation. In the Lagrangian material-based formulation, the reference is the *undeformed* centerline of the strip, denoted as the material-fixed arc length coordinate S. In the Eulerian space-based formulation, the arc length is measured along the actual *deformed* centerline of the strip, which is represented as the space-fixed arc length coordinate s. The "axial stretch" $\lambda_{11,CL}$ follows as differential mapping from the Lagrangian to the Eulerian domain at time t

$$ds = \lambda_{11,CL} \cdot dS = (1 + \varepsilon_{11,CL}) \cdot dS \tag{1}$$

and depends on the tangential centerline strain $\varepsilon_{11,CL}$. Let us now introduce a special ALE reference system with an ALE referential coordinate χ along the undeformed centerline of the strip (cp. Figure 3). The referential coordinate χ of a certain material point (described by S in the Lagrangian material-based reference system) is expressed as "particle name difference"

$$\chi(S,t) = S - S_Q(t), \tag{2}$$

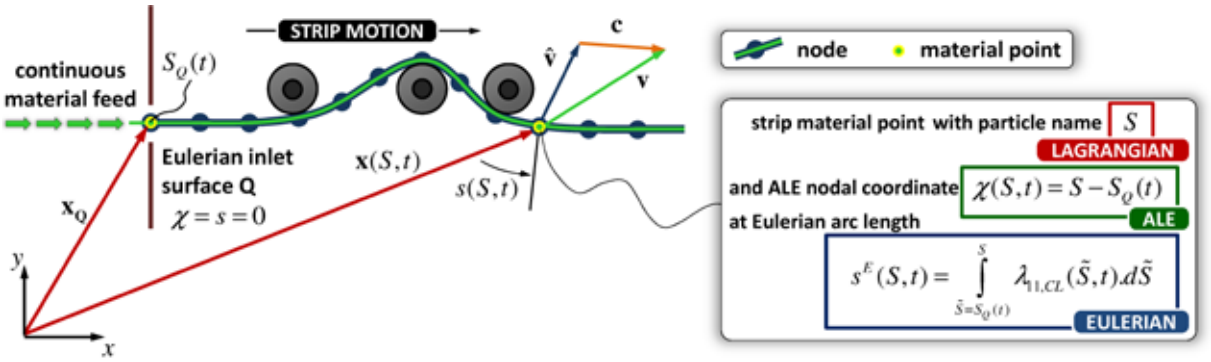

Figure 3: Correlations between Lagrangian, Eulerian and ALE referential domains.

Figure 4: Mapping between Lagrangian, Eulerian and ALE referential domains.

therefore,

$$d\chi = dS \quad \text{and} \quad \left.\frac{\partial}{\partial \chi}\right|_t = \left.\frac{\partial}{\partial S}\right|_t . \tag{3}$$

The actual position of this point along the Eulerian space-based arc length s follows from the integration of Equation 1 as

$$s(S,t) = \int_{S_Q(t)}^{S} \lambda_{11,CL}(\tilde{S},t) \cdot d\tilde{S}. \tag{4}$$

In Equations 2 and 4, $S_Q(t)$ refers to the time-dependent material-based "particle name", which – at time t – enters the system at the Eulerian (hence, space-fixed) inlet surface Q.

According to the correlations presented in [1], the function $\boldsymbol{\varphi}$ denotes the nonlinear mapping from the Lagrangian material domain to the Eulerian spatial domain, the function $\boldsymbol{\Phi}$ represents the nonlinear mapping from the ALE referential domain to the Eulerian spatial domain and the function $\boldsymbol{\Psi}$ designates the linear mapping from the ALE referential domain to the Lagrangian spatial domain (cp. Figure 4).

$$\begin{aligned} \text{Lagrangian} \rightarrow \text{Eulerian:} \quad & \boldsymbol{\varphi} : (S,t) \longmapsto \boldsymbol{\varphi}(S,t) = (s,t) \\ \text{ALE} \rightarrow \text{Eulerian:} \quad & \boldsymbol{\Phi} : (\chi,t) \longmapsto \boldsymbol{\Phi}(\chi,t) = (s,t) \\ \text{ALE} \rightarrow \text{Lagrangian:} \quad & \boldsymbol{\Psi} : (\chi,t) \longmapsto \boldsymbol{\Psi}(\chi,t) = (S,t), \end{aligned} \tag{5}$$

then the mapping $\boldsymbol{\varphi}$ can be expressed by $\boldsymbol{\Phi}$ and $\boldsymbol{\Psi}$ as

$$(s,t) = \boldsymbol{\varphi}(S,t) = \boldsymbol{\Phi}(\chi,t) = \boldsymbol{\Phi}\left(\boldsymbol{\Psi}^{-1}(S,t)\right), \tag{6}$$

with

$$\boldsymbol{\varphi}(S,t) = \begin{pmatrix} \int_{S_Q}^{S} \lambda_{11,CL}(\tilde{S},t)\cdot d\tilde{S} \\ t \end{pmatrix}, \boldsymbol{\Phi}(\chi,t) = \begin{pmatrix} \int_{0}^{\chi} \lambda_{11,CL}(\tilde{\chi},t)\cdot d\tilde{\chi} \\ t \end{pmatrix} \tag{7}$$

$$\text{and } \boldsymbol{\Psi}^{-1}(S,t) = \begin{pmatrix} S - S_Q(t) \\ t \end{pmatrix}.$$

The derivatives of $\boldsymbol{\varphi}$ with respect to the Lagrangian material based arc-length S and time t follow from Equation 6 as

$$\frac{\partial \boldsymbol{\varphi}(S,t)}{\partial(S,t)} = \frac{\partial \boldsymbol{\Phi}}{\partial(\chi,t)} \cdot \frac{\partial \boldsymbol{\Psi^{-1}}}{\partial(S,t)}, \tag{8}$$

which can be re-written in matrix notation as

$$\begin{pmatrix} \left.\frac{\partial s}{\partial S}\right|_t & v \\ 0 & 1 \end{pmatrix} = \begin{pmatrix} \frac{\partial s}{\partial \chi} & \hat{v} \\ 0 & 1 \end{pmatrix} \cdot \begin{pmatrix} \left.\frac{\partial \chi}{\partial S}\right|_t & w \\ 0 & 1 \end{pmatrix}, \tag{9}$$

with

$$\hat{v} = \left.\frac{\partial s}{\partial t}\right|_{\chi} = \int_{0}^{\chi} \left.\frac{\partial \lambda_{11,CL}}{\partial t}\right|_{\tilde{\chi}} \cdot d\tilde{\chi} \text{ and } w = \left.\frac{d\chi}{dt}\right|_{S} = -\frac{dS_Q}{dt}, \tag{10}$$

where v denotes the material speed, $\hat{v}$ represents the nodal speed and w describes the referential material velocity (i.e. the change rate of the "position" of a certain material particle S in the ALE referential coordinate system χ).

Block multiplication of Equation 9 using Equation 10 leads to

$$v = \left.\frac{\partial s}{\partial t}\right|_{S} = \hat{v} + \frac{\partial s}{\partial \chi}\cdot w = \underbrace{\int_{0}^{\chi} \left.\frac{\partial \lambda_{11,CL}}{\partial t}\right|_{\tilde{\chi}} \cdot d\tilde{\chi}}_{\substack{\text{nodal movement:} \\ \text{transient phase only}}} + \underbrace{\lambda_{11,CL}\cdot w}_{\substack{\text{transient} \\ \text{phase \&} \\ \text{steady} \\ \text{state}}}, \tag{11}$$

which can be transformed into the definition of the convective velocity c (cp. again [1]), which follows as

$$c = v - \hat{v} = \frac{\partial s}{\partial \chi} \cdot w = \lambda_{11,CL} \cdot w. \tag{12}$$

Note that the convective speed c will only coincide with w if $ds/dS = 1$, implying that the mapping is purely translational, i.e. not exhibiting any axial stretches. Furthermore, the nodal speed $\hat{v}$ will vanish under steady state conditions for this special ALE formulation, as $\partial\lambda_{11,CL}/\partial t|_{\chi\in[0,\chi_{END}]} = 0$ in a steady state. Hence, in the considered steady state, the material speed and the convective speed coincide ($v = c$). The material time derivative of a physical distribution $f = f^{LAG}(S,t) = f^{EUL}(s,t) = f^{ALE}(\chi,t)$ along the strip's bendingline can be written as

$$\frac{df}{dt} = \left(\left.\frac{\partial}{\partial t}\right|_S\right) f^{LAG} = \left(\left.\frac{\partial}{\partial t}\right|_s + v \cdot \frac{\partial}{\partial s}\right) f^{EUL} = \left(\left.\frac{\partial}{\partial t}\right|_\chi + w \cdot \frac{\partial}{\partial \chi}\right) f^{ALE}. \tag{13}$$

The ALE steady state condition follows as

$$\left.\frac{\partial f}{\partial t}\right|_\chi = \underbrace{\left(\frac{1}{\lambda_{11,CL}} \cdot v - w\right)}_{\substack{=0 \text{ in the steady state} \\ \text{for this special ALE formulation}}} \cdot \frac{\partial f}{\partial \chi}, \tag{14}$$

which illustrates that the time derivatives at any ALE reference coordinate χ must vanish in the considered steady state employing the presented special ALE description.

In special physical scenarios, the presented ALE formulation may be directly transformed either into a purely Lagrangian or into a purely Eulerian formulation.

For the *Lagrangian formulation*, $S_Q(t) = const.$ In this case, the derivative $\partial\boldsymbol{\Psi}^{-1}/\partial(S,t)$ reduces to the identity matrix $\boldsymbol{I}$ and Equation 8 turns into $\partial\boldsymbol{\varphi}/\partial(S,t) = \partial\boldsymbol{\Phi}/\partial(\chi,t)$, which requires that $\chi \equiv S - const.$ The ALE domain changes into a purely Lagrangian formulation, where the material referential velocity as well as the convective velocity are zero ($w = c = 0$), and the material speed and the mesh speed coincide ($v = \hat{v}$).

In the *Eulerian formulation*, $ds/d\chi = \lambda_{11,CL} = 1$ and $\chi \equiv s$. Analogously to above, the derivative $\partial\boldsymbol{\Phi}/\partial(S,t)$ reduces to the identity matrix $\boldsymbol{I}$ and Equation 8 turns into $\partial\boldsymbol{\varphi}/\partial(S,t) = \partial\boldsymbol{\Psi}^{-1}/\partial(S,t)$. For this special case, the ALE domain changes into a purely Eulerian formulation, where the actual material speed v equals both the convective speed c and the material referential velocity w ($v = c = w$), and where the mesh speed $\hat{v}$ is zero ($\hat{v} = 0$) even in the transient phase of the simulation.

6 PARAMETERIZATION

Appropriate *Parametric Shape Functions* are essential both for the strip curvature κ and the centerline strain $\varepsilon_{11,CL}$ distributions

$$\kappa = \frac{d\theta}{ds} \quad \text{and} \quad \varepsilon_{11,CL} = \lambda_{11,CL} - 1 = \left\| \frac{d\boldsymbol{x}}{d\chi} \right\| - 1, \tag{15}$$

where θ denotes the strip section angle and $\boldsymbol{x}(\chi)$ the strip centerline in real space. The section angle θ determines the direction of the strip's tangential unit vector $\hat{\boldsymbol{t}} = (cos\theta, sin\theta)^T$ as well as of the strip's normal vector $\hat{\boldsymbol{n}} = (-sin\theta, cos\theta)^T$. The Bernoulli-Euler beam theory is applied here, which requires that plane strip cross-sections remain plane and normal to the strip centerline throughout the deformation.

The nodal interpolation scheme (i.e. the order of the shape functions used in-between the parametric sampling points at the nodes) must be chosen carefully to comply with the fundamental correlations of the local equilibrium conditions in curved rods. As outlined in [8], the distribution of the bending moment $M(s)$ along the actual Eulerian arc length s must be continuous within the process unit of a tension leveler, however, the first derivative dM/ds of the bending moment with respect to the arc length, as well as the shear force distribution $F_{12}(s)$ are typically discontinuous at the contact areas. The distribution of the concentrated tangential strip force $F_{11}(s)$ is typically continuous, if the rolls are not driven.

Presuming a continuous, path-dependent, elasto-viscoplastic constitutive law (excluding special phenomena like a pronounced yield strength, recrystallization processes, crack formations, etc.), then arbitrarily small tangential strip force and bending moment variations are the result of arbitrarily small cross-section strain variations. In this case, the continuity condition of the bending moment distribution $M(s)$ can be extended to the strip curvature distribution $\kappa(s)$, and the continuity condition of the tangential force distribution $F_{11,CL}(s)$ also applies to the strip centerline strain distribution $\varepsilon_{11,CL}$.

7 PRINCIPLE OF VIRTUAL WORK

The *principle of virtual work* is employed in order to identify the parameter set that matches the solution. Only for this parameter set, the virtual internal strain energy δU equals the virtual work of the external forces δW, hence, the principle of virtual work can be written as

$$\delta U - \delta W = 0 = \sum_{i=1}^{n} \delta P_i \cdot \Bigg(\underbrace{\int_0^{l_0} \left(F_{11} \cdot \frac{\partial \varepsilon_{11,CL}}{\partial P_i} + M \cdot \frac{\partial \kappa}{\partial P_i} \right) \cdot d\tilde{\chi}}_{\text{virt. internal strain energy}} - \tag{16}$$

$$- \underbrace{\sum_{j=1}^{k} \mathbf{F}_{\mathbf{EXT},j} \cdot \frac{\partial \mathbf{x}_{\mathbf{EXT},j}}{\partial P_i}}_{\text{virt. work of external forces}} - \underbrace{\int_0^{l_0} \left(\mathbf{q} \cdot \frac{\partial \mathbf{x}}{\partial P_i} \right) \cdot d\tilde{\chi}}_{\text{virt. work of distr. loads}} \Bigg),$$

where P_i denote the shape function parameters ($i \in [1, n]$, with n parameters in total), l_0 represents the modeled, undeformed strip length ($\chi \in [0, l_0]$), $\boldsymbol{F_{EXT,j}}$ (with $j \in [1, k]$) designate the concentrated external forces at the material points $\boldsymbol{x_{EXT,j}}$ and $\boldsymbol{q}(\chi)$ represents the distributed loads along the bending line $\boldsymbol{x}(\chi)$. Distributed loads may arise from inertial and gravitational effects and can be computed as

$$\boldsymbol{q}(\chi) = -\varrho^*(\chi) \cdot \left(\hat{\boldsymbol{e}}_y \cdot g + \hat{\boldsymbol{n}}(\chi) \cdot v(\chi)^2 \cdot \kappa(\chi)\right), \tag{17}$$

where ϱ^* denotes the local mass per unit of strip length ($\varrho^*(\chi) = \varrho \cdot b \cdot h(\chi)$ – with strip width b and strip thickness h), where $\hat{\boldsymbol{e}}_y$ represents the unit vector in the global y-direction, and where g stands for the gravitational constant.

8 CONTACT FORMULATION

In order to include nodal contact into the principle of virtual work, the undisturbed system is extended by a contact term δW_C (hence, $\delta U - \delta W - \delta W_C = 0$).

Strip/roll contact is established at selected nodes by employing the Lagrange Multiplier method. A contact identification algorithm detects those nodes that penetrate one of the rolls. At these nodes, contact forces are determined by the additional Lagrangian parameter $\lambda_{C,a}$ ($a \in [1, c]$ for c contact nodes).

The contribution to the virtual work can be written as

$$\delta W_C = \sum_{i=1}^{n} \delta P_i \cdot \left(\sum_{a=1}^{c} \left(\boldsymbol{F_{C,a}} \cdot \frac{\partial \boldsymbol{x_C}(\chi_a)}{\partial P_i} + \frac{\partial \boldsymbol{F_{C,a}}}{\partial P_i} \cdot \boldsymbol{c}_a \right) \right), \tag{18}$$

where the nodal contact force $\boldsymbol{F_{C,a}}$ must be normal to the strip centerline, as frictionless strip/roll contact is assumed

$$\boldsymbol{F_{C,a}} = \lambda_{C,a} \cdot \hat{\boldsymbol{n}}(\chi_a) \text{ and } \frac{\partial \boldsymbol{F_{C,a}}}{\partial P_i} = \frac{\partial \lambda_{C,a}}{\partial P_i} \cdot \hat{\boldsymbol{n}}(\chi_a) - \lambda_{C,a} \cdot \frac{\partial \theta}{\partial P_i} \cdot \hat{\boldsymbol{t}}(\chi_a). \tag{19}$$

The contact condition $\boldsymbol{c}_a$ (i.e. the side condition for the geometric distance, which vanishes when the contact is established) can be written as the following kinematic constraint

$$\boldsymbol{c}_a = \boldsymbol{x_{C,a}} - \boldsymbol{x_{R,a}} - \varpi_a \cdot r_a \cdot \hat{\boldsymbol{n}}(\chi_a), \tag{20}$$

where $\boldsymbol{x_{C,a}}$ denotes the position of the node in contact, $\boldsymbol{x_{R,a}}$ the center of the respective roll in contact, $\varpi_{,a}$ the contact orientation ($\varpi_a = 1$ if the strip normal vector $\hat{\boldsymbol{n}}(\chi_a)$ points in the direction of the respective roll's center point, and $\varpi_a = -1$ if $\hat{\boldsymbol{n}}(\chi_a)$ points into the opposite direction) and where r_a represents the respective roll radius.

9 PRESENTATION OF SELECTED RESULTS

A self-developed and customized simulation prototype (implemented in MATLAB$^{\text{TM}}$) can now be used instead of computationally expensive FEM simulations (based on commercial Finite Element packages). The CPU times for typical tension leveling scenarios

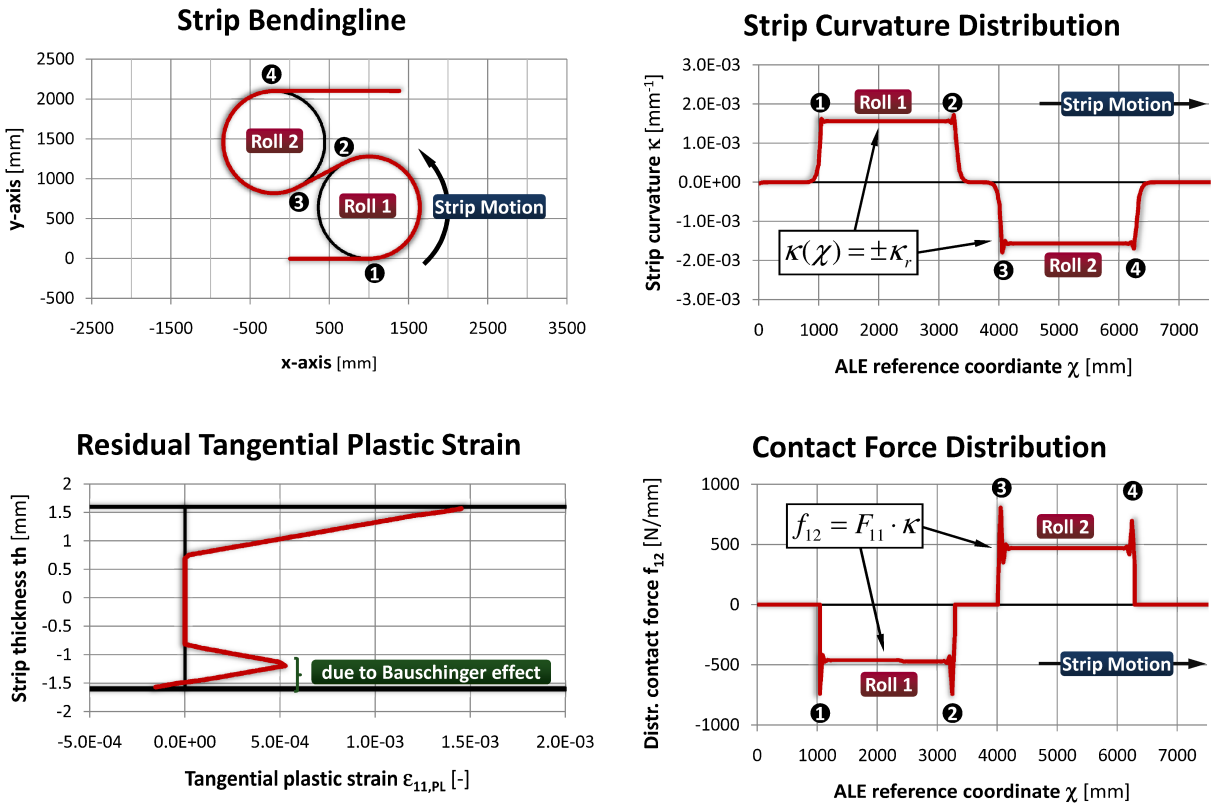

Figure 5: Selected results for surface contact scenarios, in which strip exhibits surface contact.

could be reduced from some days (using commercial Finite Element packages) to a few minutes (employing the self-developed PSF model).

Due to the advantageous parameterization along the referential ALE arc length of the bending line, large strip rotations (of more than 180°) can be handled without any problem. Both *line contact* (where the peak curvature of the strip is smaller than the curvature of the respective roll and therefore has to follow from the simulation) and *surface contact* (where the strip's curvature adopts the curvature of the respective roll) can be handled by the implemented contact algorithm.

Figure 5 depicts the simulation results of a roll unit, where metal strip is deflected under high tension around two undriven rolls of large diameters. From the strip bending line (top left image in Figure 5) it follows that the strip is deflected twice by more than 180° as it runs around the rolls. The strip curvature distribution diagram (top right image in Figure 5) exhibits the typical plateaus, where the strip's curvature is restricted by the curvature of the roll as upper bound (the roll radius is 640 mm in this case, hence the strip's curvature cannot exceed $1.6 \cdot 10^{-3}$ mm^{-1}). The bottom left diagram in Figure 5 depicts the residual strain distribution across the strip thickness, after the strip was bent twice around both rolls. Note that the plastic compression at the bottom strip surface

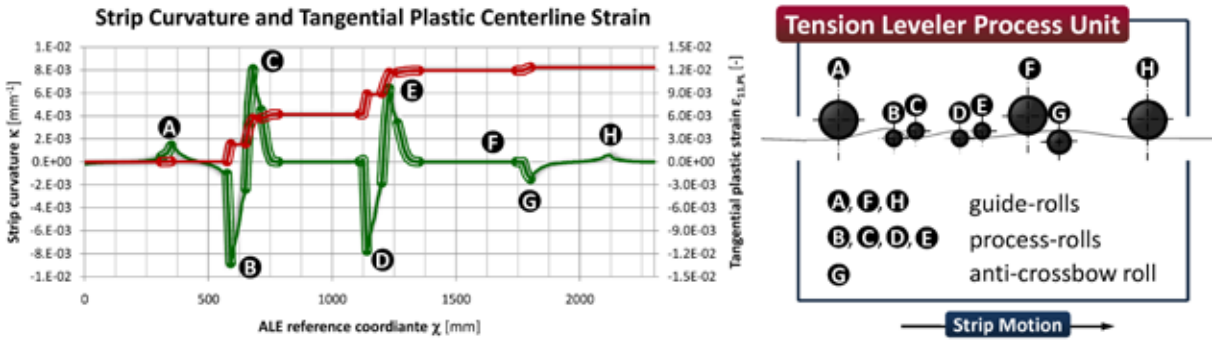

Figure 6: Strip curvature and tangential plastic centerline strain for a typical tension leveling scenario.

is due to the consideration of the material's Bauschinger effect: after first elasto-plastic strains have occurred at the strip bottom surface fibers (near the contact point with roll 1), the yield strength of the material is reduced when the direction of the deformation is inverted from tension to compression (at roll 2). The contact force distribution diagram (bottom right image in Figure 5) clearly displays the single contact force peaks at the beginning and at the end of each strip/roll contact (labels 1 - 4) as well as the evenly distributed sectional shear force f_{12} (proportional to the roll radius and the tangential strip force F_{11} – cp. [8]) within the surface contact zone.

Figure 6 illustrates some simulation results of typical strip deformations within the process unit of an industrial tension leveler. The red line illustrates the tangential strip strain distribution, the green line shows the strip curvature distribution. Those strip segments along the bending line, which exhibit plastic deformation, are highlighted as bold lines. It becomes obvious that the largest tangential plastic strains occur within the curved strip segments before the process-rolls (labels "B", "C", "D" and "E" in Figure 6). Minor plastifications can be observed after process-rolls "C" and "E" as well as near guide-roll "A" and anti-crossbow roll "G". From Figure 6 it becomes obvious, that less than 20 % of the strip length in the process unit are deformed plastically in typical steady state scenarios of the tension leveling process.

10 CONCLUSIONS

A thorough analysis of the physical correlations and mechanical aspects of tension leveling scenarios is essential for the reliable and accurate design of the tension leveling processes, machines and controls. The presented self-developed simulation prototype is based on a special Arbitrary Lagrangian-Eulerian formulation and employs the Principle of Virtual Work. Due to its optimized simulation algorithms and the decoupling of the nodal from the material movement, it allows for short simulation runtimes (within the range of a few minutes).

The model is currently used in large-scale parametric studies in the design phase of industrial tension levelers. The direct benefits gained from the model are minimized plant

investments, better plant performance as well as a reduction of energy costs.

ACKNOWLEDGEMENT

This research project was carried out within the framework of the "Austrian Center of Competence in Mechatronics" (ACCM), a K2 center of the COMET program, which is carried out by FFG and is supported by the Austrian Federal Government (the Federal Ministry for Transport, Innovation and Technology and the Federal Ministry of Economy, Family and Youth), by the Province of Upper Austria, as well as by the Company Partners and Scientific Partners of ACCM.

The authors gratefully acknowledge the continuous and comprehensive support of Siemens VAI in this research project.

REFERENCES

[1] Donea, J., Huerta, A., Ponthot, J.Ph. and Rodríguez-Ferran, A., Arbitrary Lagrangian-Eulerian methods. *Encyclopedia of Computational Mechanics.* (2004).

[2] Kulbatschny, I.G., *Maschinelle Ausrüstung von Walzwerken (German).* VEB Verlag Technik Berlin, (1954).

[3] Sheppard, T. and Roberts, J.M. On the Strip-to-Roll Conformity in the Tension-Leveling Process. *Journal of the Institute of Metals* (1972): 130–135.

[4] Misaka, Y. and Masui T., Shape Correction of Steel Strip by Tension Leveler. *Transaction ISIJ* (1977) **18**:475-484.

[5] Hoffmann, J., *Simulationsmodell für das Streckbiegerichten (German).* PhD-thesis, Magdeburg, (1996).

[6] Steinwender, L., Salzmann, C., Kainz, A., Krimpelstätter, K. and Zeman, K., A Holistic Modeling Approach for the Design of Tension Leveling Processes and Equipment. *Proceedings SHEMET Leuven/Belgium. Key Engineering Materials* (2011) **473**:757-764.

[7] Steinwender, L., Kainz, A., Krimpelstätter, K. and Zeman, K., Computational Analysis of the Curvature Distribution and Power Losses of Metal Strip in Tension Levellers. *Proceedings WCCM/APCOM Sydney/Australia. IOP Conf. Ser.: Mater. Sci. Eng.* (2010) **10**.

[8] Steinwender, L., Kainz, A., Krimpelstätter, K. and Zeman, K., A Novel Approach for Modeling of the Tension Leveling Process by Employing Parametric Shape Functions. *Proceedings STEELSIM Düsseldorf/Germany* (2011).